HHS Public Access

Author manuscript

Cell. Author manuscript; available in PMC 2017 May 19.

Published in final edited form as:

Cell. 2016 May 19; 165(5): 1147–1159. doi:10.1016/j.cell.2016.04.002.

A tension based model distinguishes hypertrophic versus dilated cardiomyopathy

Jennifer Davis[1], **L. Craig Davis**[2], **Robert N. Correll**[3], **Catherine A. Makarewich**[4], **Jennifer A. Schwanekamp**[3], **Farid Moussavi-Harami**[1], **Dan Wang**[1], **Allen J. York**[3], **Haodi Wu**[5], **Steven R. Houser**[4], **Christine E. Seidman**[6], **Jonathan G. Seidman**[6], **Michael Regnier**[1], **Joseph M. Metzger**[7], **Joseph C. Wu**[5], and **Jeffery D. Molkentin**[3,8,*]

[1]Department of Bioengineering, University of Washington, Seattle, WA, USA

[2]10244 Normandy Dr., Plymouth MI, USA

[3]Cincinnati Children's Hospital Medical Center, Department of Pediatrics, University of Cincinnati, Cincinnati, OH, USA

[4]Department of Physiology, Temple University, Philadelphia, PA, USA

[5]Stanford Cardiovascular Institute, Stanford University School of Medicine, Stanford, CA, USA

[6]Department of Genetics, Harvard Medical School, Division of Cardiovascular Medicine, Brigham and Women's Hospital, Boston, MA, USA

[7]Department of Integrative Biology and Physiology, University of Minnesota Medical School, Minneapolis, MN, USA

[8]Cincinnati Children's Hospital Medical Center, Howard Hughes Medical Institute, Cincinnati, OH, USA

SUMMARY

The heart either hypertrophies or dilates in response to familial mutations in genes encoding sarcomeric proteins, which are responsible for contraction and pumping. These mutations typically alter calcium-dependent tension generation within the sarcomeres, but how this translates into the spectrum of hypertrophic versus dilated cardiomyopathy is unknown. By generating a series of cardiac-specific mouse models that permit the systematic tuning of sarcomeric tension generation

[*]Correspondence: ; Email: jeff.molkentin@cchmc.org.

SUPPLEMENTAL INFORMATION

Supplementary information includes 7 figures and an Extended Experimental Methods section:

AUTHOR CONTRIBUTIONS

J.D.M., J.D., M.R., and S.R.H conceived and designed the study. Experiments were performed by J.D., D.W., A.J.Y., J.A.S., F M-H., C.A.M., R.N.C., and H.W. L.C.D and J.D. generated the computational model. C.E.S and J.G.S. provided the Myh6-403 mouse and critical feedback on the manuscript. J.M.M provided feedback on the study and written manuscript, as well as the cTnI adenovirus and stimulation chambers. J.C.W and H.W provided data in cardiomyocytes generated from human iPSCs from patients with HCM or DCM. J.D.M and J.D. wrote the manuscript with input from all authors.

Conflict of interest: None (no competing financial interests).

and calcium fluxing, we identify a significant relationship between the magnitude of tension developed over time and heart growth. When formulated into a computational model the integral of myofilament tension development predicts hypertrophic and dilated cardiomyopathies in mice associated with essentially any sarcomeric gene mutations, but also accurately predicts human cardiac phenotypes from data generated in induced-pluripotent stem cell-derived myocytes from familial cardiomyopathy patients. This tension-based model also has the potential to inform pharmacologic treatment options in cardiomyopathy patients.

INTRODUCTION

Inherited cardiomyopathy defines a heterogeneous group of heart muscle diseases that affects 1:500 people in the general population (McNally et al., 2013). There are two primary clinical phenotypes that include hypertrophic (HCM) and dilated (DCM) cardiomyopathy. Morphologically, HCM is characterized by asymmetric heart growth with a reduction in ventricular chamber dimension, thickening of the interventricular septum and diastolic dysfunction with an increased risk of sudden cardiac death due to arrhythmia (Fatkin and Graham, 2002). By comparison, DCM is defined by an enlarged left ventricular chamber that is accompanied by a type of dilated or eccentric “hypertrophy” in which myocytes typically lengthen resulting in reduced systolic function (McNally et al., 2013). In either case there is no cure for these 2 disease states with the only effective long-term treatment being transplantation (Tardiff et al., 2015).

Familial HCM and DCM arise from nearly 1500 distinct mutations in the genes that encode for proteins of the sarcomere (McNally et al., 2013). The sarcomere is the basic unit in muscle that generates tension and subsequent contraction through a process known as excitation-contraction coupling. In the heart, depolarization of the muscle cell membrane results in Ca^{2+} influx through sarcolemmal L-type Ca^{2+} channels that then induces a much larger release of Ca^{2+} from the intracellular sarcoplasmic reticulum (SR) network. This Ca^{2+} then binds the sarcomeric protein cardiac troponin C (cTnC) to initiate crossbridge cycling between myosin and actin, which then generates force and cellular shortening (Bers, 2002). During relaxation Ca^{2+} is transported back into the SR by the SR Ca^{2+} ATPase2 (SERCA2), which lowers cytosolic Ca^{2+} allowing for increased Ca^{2+} dissociation from cTnC and a reduction in crossbridge adherence and sarcomeric tension (Bers, 2002; Gordon et al., 2000).

Sarcomeric gene mutations typically disrupt the highly tuned balance between mechanical force generation and Ca^{2+} cycling dynamics. For example, HCM-related mutations sensitize the myofilaments towards greater Ca^{2+} adherence thereby prolonging mechanical relaxation and delaying Ca^{2+} reuptake into the SR. DCM-linked mutations typically desensitize the myofilaments to Ca^{2} requiring higher levels of free cytosolic Ca^{2+} for tension generation, and Ca^{2+} more rapidly dissociates from the sarcomere during relaxation. However, it is unknown how such mutations program a continuum of cardiac remodeling from severe hypertrophic growth with myocyte thickening to extreme dilation and cellular lengthening (Kehat and Molkentin, 2010; McNally et al., 2013). A lack of such understanding makes it difficult to predict clinical outcomes of genotyped patients with standard of care medications

used in the heart failure setting. Indeed, pediatric patients with familial HCM appear to do worse when treated with Ca^{2+} channel blockers (Ostman-Smith, 2010), and β-adrenergic receptor blockers do not reduce adult HCM disease progression and hypertrophy (Hamada et al., 2014; Spoladore et al., 2012).

Using an array of genetically altered mice we systematically altered the Ca^{2+}-tension relationship *in vivo* with quantifiable changes in either myofilament tension generation or Ca^{2+} transient kinetics to assess the ramifications on cardiac remodeling and disease. Experimental data from this approach was used to develop a mathematical index that predicts if the heart will undergo either hypertrophic or dilated cardiac growth through 2 signaling pathways that directly interpret the area under the tension/shortening curve. This index also predicts the type of cardiac growth associated with select pharmacotherapies in mice with simulated HCM or DCM mutations in sarcomeric proteins. Moreover, the tension-index calculated from human HCM and DCM cardiac myocytes derived from induced-pluripotent stem cells (iPSCs) accurately predicts a patient's known clinical phenotype.

RESULTS

Altering Myofilament Ca^{2+} Sensitivity *in vivo* With Designed cTnC Variants

It remains unclear how mutations in sarcomeric genes mediate differential heart growth typical of familial HCM and DCM. Two diametrically opposed cTnC (*Tnnc1* gene) variant proteins were used that quantitatively shift Ca^{2+} binding and tension producing characteristics of the myofilaments at a set amount on either side of normal to correlate with cardiac structural remodeling (Kreutziger et al., 2011; Tikunova and Davis, 2004). Isolated adult rat cardiomyocytes were first infected with recombinant adenovirus encoding β-galactosidase (βgal, control for virus infection) and Flag epitope-tagged wild-type (WT), L48Q or I61Q cTnC mutants. At 3 days post infection approximately 50% of endogenous cTnC was replaced with either the Flag-tagged WT, L48Q or I61Q cTnC, without changes in other sarcomeric proteins like tropomyosin (Tm) or α-actinin (Figure 1A). Moreover, there was no difference in the relative expression of the cTnC variants between intact and fully permeabilized myocytes suggesting that the Flag-tagged cTnC constructs were incorporating into the sarcomeres (Figure 1A). Indeed, co-immunoprecipitating (IP) the troponin complex with anti-cTnT demonstrated that the two Flag-tagged mutants were each incorporated into the troponin complex at roughly the same level (Figure 1B).

In myocyte contractile assays, L48Q cTnC significantly increased cellular fractional shortening in the absence of changes in Ca^{2+} transient amplitude (*data not shown*), as previously reported (Feest et al., 2014). Acute expression of I61Q cTnC caused a modest reduction in fractional shortening with no changes in Ca^{2+} transient amplitude reflecting the decreased sensitivity of the myofilaments to Ca^{2+} (*data not shown*). In terms of kinetics, L48Q cTnC significantly slowed myocyte relaxation and Ca^{2+} decay, while I61Q cTnC accelerated both of these parameters (Figure 1C & D). Together these data suggest that sarcomeric incorporation of the L48Q or I61Q cTnC variants effectively redistributes Ca^{2+} either onto the sarcomere to enhance tension generation (L48Q cTnC) or freely into the cytosol thereby decreasing overall tension generation (I61Q cTnC).

To understand the *in vivo* consequence associated with directionally adjusting myofilament Ca^{2+}-mechanical coupling, transgenic mice (TG) were generated with cardiac-specific expression of L48Q, I61Q, or WT cTnC using a tetracycline bi-transgenic inducible system (Figure 1E). All of the constructs were tagged with a Flag epitope to determine percent replacement with the transgene-encoded protein (Figure 1E). Previous work demonstrated that expression of an epitope tagged cTnC is innocuous (Davis and Metzger, 2010). Replacement of the endogenous cTnC with the epitope-tagged versions was assessed by western blotting at 1 month of age (Figure 1F). Overexpression of WT, L48Q, and I61Q cTnC in mice averaged 50%, 40%, and 45% stoichiometric replacement, respectively (Figure 1F, slower migrating band is Flag-tagged). In the absence of the tTA (tetracycline transactivator) transgene, both the L48Q and I61Q responder lines had a minor degree of leak resulting in 5–10% replacement at baseline (Figure 1F). The inducibility feature of this bi-transgenic system was not employed given that constitutive expression of cTnC WT and the 2 variants did not reduce birth rates of the mice.

Using data from these cTnC expressing TG mice we refined an existing computational model of myocyte contraction to simulate Ca^{2+} transients and tension dynamics (Negroni and Lascano, 2008). These simulations predicted that L48Q prolongs the time a myocyte experiences elevated tension with a set amount of Ca^{2+}, as well as slowed relaxation, while I61Q reduced tension and hastened relaxation for the same amount of Ca^{2+} (Figure 1G & H). Relative to WT, the L48Q Ca^{2+} transient also had slower decay kinetics, while the I61Q variant invoked a greater transient with a shortened decay time (Figure 1H). A linear regression analysis was used to assess how accurately values from the Ca^{2+} and myocyte shortening simulations predicted actual values from the cTnC variants, and in both cases the R^2 values were significant and greater than 0.6 suggesting a strong correlation (Figure S1A–D). Together these simulations suggested a highly integrated relationship between changes in myofilament Ca^{2+} sensitivity and tension production with reflexive changes in the Ca^{2+} transient to maintain a contractile set-point.

L48Q cTnC Predisposes to Hypertrophic Remodeling

Cardiac myocytes isolated from L48Q mice had increased fractional shortening despite smaller Ca^{2+} amplitudes compared with control myocytes, confirming that this mutation enhances myofilament Ca^{2+} sensitivity (Figure 2A & B). L48Q myocytes also had significantly slower relaxation and rate of Ca^{2+} transient decay in comparison to the tTA and WT cTnC controls (Figure 2C & D). Despite prolonged relaxation, L48Q TG mice had hyperfunctional hearts (Figure 2E) with no change in cardiac growth or chamber dimensions up to 1 year of age (Figure 2F–I).

There are other examples of TG and knock-in mouse models of HCM that fail to phenocopy the asymmetric hypertrophic thickening of the myocardium observed in HCM patients, even independently generated L48Q TG mice (Shettigar et al., 2016; Davis et al., 2012; Michele et al., 2002). Thus, we hypothesized that the effects of L48Q cTnC are masked by the known high adrenergic drive and heart rate of the mouse, which accelerates diastolic function through increasing Ca^{2+} reuptake by SERCA2 and desensitizing the sarcomere to Ca^{2+} by phosphorylating the amino terminal serine residues (23/24) on cTnI (Metzger and Westfall,

2004). We reasoned that tempering the adrenergic state of the mouse with chronic delivery of the β-receptor antagonist, metoprolol, might unmask the effects of L48Q cTnC *in vivo*. While 3 months of metoprolol treatment in L48Q TG mice had no effect on systolic performance (Figure 2J), these mice now developed significant heart remodeling in which both the left ventricular (LV) chamber dimension, septal wall thickness and cardiac mass became significantly larger (Figure 2K–N). In contrast, metoprolol delivery to tTA control mice had negligible effects on ventricular performance or cardiac remodeling (Figure 2J–N).

Because the effects of metoprolol were unexpected, we repeated this entire experimental paradigm using adeno-associated virus serotype 6 (AAV) to overexpress either WT cTnC or L48Q cTnC in mice for the first time at 8 weeks of age (each was Flag-tagged). Infected mice were then given metoprolol-treated water for 1 month. This *in vivo* gene-transfer strategy produced 50–60% and 40–50% replacement of native cTnC with WT cTnC and L48Q cTnC, respectively (Figure S2A). Similar to results in the TG mice, the acutely infected L48Q mice developed a significant increase in septal and posterior wall thickness, as well as increased ventricular mass with metoprolol administration, while WT AAV-cTnC expressing mice showed no effect (Figure S2B–D). Consistent with this profile, acute metoprolol treatment further slowed L48Q cellular relaxation time and Ca^{2+} re-uptake in isolated cardiomyocytes, an effect that was also seen in tTA control myocytes, albeit to a lesser extent (Figure 2O & P).

To further examine this effect observed with β-blockers a cohort of AAV-infected WT cTnC and L48Q mice were also chronically treated with the SA-node antagonist ivabradine (10 mg/kg/day) to decrease chronotropy and increase the time in diastole. Similar to the effects of β-blockers, ivabradine-treatment caused a mild hypertrophic growth of the septal and posterior walls and increased cardiac mass in L48Q-infected mice, but not in WT cTnC infected mice (Figure S2E–G). Together these data suggest that prolonging mechanical tension initiates growth signaling, which in the mouse is compensated by an increase in sympathetic drive.

The converse experiments were also performed in which the high adrenergic drive of the mouse was mimicked in isolated myocytes by applying the β-adrenergic agonist isoproterenol. As expected, isoproterenol corrected the slowed relaxation and Ca^{2+} decay times in L48Q myocytes to vehicle-treated tTA values (Figure 2O & P). To corroborate these data, the Ca^{2+} binding affinity of cTnC and L48Q cTnC were examined in the presence of phosphorylated or non-phosphorylated cTnI using steady-state fluorescence spectroscopy. Phosphorylated cTnI caused a decreased Ca^{2+} binding affinity of both WT cTnC and L48Q cTnC, as indicated by the rightward shift in binding fluorescence for a given Ca^{2+} concentration (pCa, Figure 2Q). Similar to the cell shortening assay, phosphorylated cTnI normalized L48Q cTnC Ca^{2+} binding affinity back to WT with non-phosphorylated cTnI levels (Figure 2Q).

L48Q mice were also subjected to 2 weeks of transverse aortic constriction (TAC) to induce pressure overload on the heart, which increased ventricular fractional shortening in control mice but had little effect on L48Q mutant mice that were already hyperfunctional (Figure 2R). While pressure overload induced hypertrophy in control mice (tTA), it produced

significantly greater hypertrophy in L48Q mice (Figure 2S & T), suggesting that greater Ca^{2+} binding to the sarcomeric regulatory proteins predisposes the heart to the hypertrophic growth response, which likely occurs by further increasing the net tension of the myofilaments.

I61Q cTnC Induces Dilated Heart Growth

The I61Q TG mouse has decreased Ca^{2+} myofilament binding affinity (Kreutziger et al., 2011), thereby recapitulating what might happen in familial DCM. I61Q TG mice have reduced myocyte shortening despite a compensatory increase in the Ca^{2+} transient amplitude when compared with tTA control myocytes (Figure 3A & B). I61Q mutant myocytes also show faster relaxation times and Ca^{2+} decay kinetics compared to tTA myocytes (Figure 3C & D). At baseline myocytes from I61Q TG mice have significantly elongated sarcomeres compared to tTA controls (Figure 3E), which is consistent with a general decrease in thin filament activation despite increased diastolic Ca^{2+} concentration (Figure 3F). *In vivo*, I61Q cTnC TG mice showed reduced cardiac function (Figure 3G & H) and a dilated phenotype characterized by increased diastolic LV chamber dimension and decreased septal wall thickness compared to age-matched tTA littermates (Figure 3I–K). Hearts harvested from I61Q mice also had increased cardiac mass (Figure 3L) and increased myocyte length-to-width ratios, suggestive of dilated eccentric growth remodeling (Figure 3M & N). These mice also have early mortality in which a substantial fraction of the cohort died by 4 months of age with no mouse surviving beyond 8 months (Figure 3O). Due to the early mortality of these mice all of the aforementioned measurements were made at 6–8 weeks of age.

Enhancing Myofilament Crossbridge Binding Corrects I61Q Disease

Since the I61Q mutation reduces myofilament tension we reasoned that a competing sarcomeric mutation that increased myofilament tension might nullify the disease effect. Hence, we employed a well characterized mouse model of HCM due to a mutation in *Myh6* at position 403 (R403Q) that promotes more time in a force generating state with prolonged relaxation (Geisterfer-Lowrance et al., 1996). I61Q TG offspring heterozygous for the R403Q mutation showed significantly improved fractional shortening, reduced left ventricle chamber dilation and normalization of septal thickness but no change in LV wall thickness (Figure 4A–D). Remarkably, I61Q-R403Q$^{+/-}$ mice showed a 40% reduction in overall heart growth when compared to the I61Q TG mice alone (Figure 4E & G). The presence of R403Q mutant *Myh6* allele also prolonged the survival of I61Q mice collectively demonstrating that enhancing the tension producing qualities of the myofilaments in “trans” could partially compensate for less cTnC Ca^{2+} binding (Figure 4F).

Directional Shifts in Ca^{2+}-Tension Underlie Cardiac Growth

The correction of I61Q-dependent dilated heart growth with the R403Q mutant myosin allele suggests that the myocyte changes its growth characteristics by sensing deviations in the time and magnitude of tension generated at a given cytosolic Ca^{2+} concentration. To examine this hypothesis we computationally simulated the twitch-force and Ca^{2+} transient for myocytes that have rapid Ca^{2+} dissociation from the sarcomere due to the combined effects of I61Q cTnC and enhanced SR Ca^{2+} reuptake. Biologically this can be achieved by increasing the Ca^{2+} binding affinity of SERCA2 through the loss of its regulatory protein,

phospholamban (*Pln* gene). Our model predicts that such an increase in SERCA2 activity would reduce the time for tension generation (Figure 5A, I61Q-*Pln*$^{-/-}$) at a given load of cytosolic Ca^{2+} in I61Q cTnC mice (Figure S3A), thus producing even greater dilated hypertrophic growth. In the context of L48Q cTnC this same enhancement in SERCA2 activity, due to loss of phospholamban, is predicted to reduce tension time and hasten the Ca^{2+} transient decay, thereby correcting the tension-Ca^{2+} transients towards WT (tTA) values (Figure 5B & S3B).

To experimentally verify the model's predictions, I61Q and L48Q TG mice were crossed with *Pln*$^{-/-}$ mice. Loss of phospholamban had no cardiac growth effect on the benign phenotype of L48Q mice, with respect to LV chamber size, septal thickness or overall heart weight (Figure 5C–E). However, loss of phospholamban did cause greater cardiac hypertrophy with increased septal thickness and overall heart weight in I61Q TG mice as predicted (Figure 5C–E). Contractile measurements made in myocytes isolated from I61Q-*Pln*$^{-/-}$ mice showed faster mechanical relaxation and Ca^{2+} transient decay times compared to I61Q myocytes, as predicted with our computational simulations (Figure S3C & S3D). Hence, loss of *Pln*$^{-/-}$ in I61Q mice further accelerated Ca^{2+} transient decay thereby exacerbating the tension deficits in an already tension poor genetic background, which correlated with greater disease and remodeling.

Using an opposing approach we simulated the effects of decreasing SERCA2 pump function in the context of I61Q and L48Q cTnC mutant phenotypes, which was compared to data in *Atp2a2* (SERCA2a) heterozygous mice. Here the model predicts that increasing the time of free cytosolic Ca^{2+} due to reduced activity of SERCA2, in the presence of the I61Q mutation, would augment the time-force production relationship, thereby partially protecting from dilated growth in I61Q mice (Figure 5F & S3F). In contrast decreasing SERCA2 activity in the presence of L48Q cTnC more than doubled the area under the tension curve and Ca^{2+} transient in comparison to simulations run with just L48Q, slowing mechanical and Ca^{2+} decay (Figure 5G & S3G). Indeed, experimental data from I61Q-*Atp2a2*$^{+/-}$ mice showed significantly reduced ventricular chamber dilation, although without a change in LV wall or septal thicknesses or heart weights (Figure 5H–K). The lack of a decrease in absolute heart weight appears to be due to a shift in the cardiac growth profile from a dilated program to more of a concentric hypertrophic program. In comparison, reduction in SERCA2 activity in the L48Q cTnC TG background produced a thickening hypertrophic response for the first time, as measured by LV wall and septal thicknesses and greater overall heart weights without a change in LV chamber size (Figure 5H–K). Together with the data observed in *Pln*$^{-/-}$ mice, the overall results suggest that altered myofilament Ca^{2+} binding properties are directly linked to SR Ca^{2+} fluxing and total free cytosolic Ca^{2+} within the cardiomyocyte, as suggested by a previously proposed disease sensing mechanism (Fatkin et al., 2000).

Tension-Ca^{2+} Growth through Calcineurin and ERK1/2 Signaling

An important regulator of heart growth is through the Ca^{2+}-responsive serine-threonine phosphatase calcineurin and its downstream transcriptional effector nuclear factor of activated T-cells (NFAT) (Houser and Molkentin, 2008). Feline cardiac myocytes were adenovirally infected with both I61Q cTnC and an NFATc3-GFP reporter for 3 days to

achieve ~60% replacement of native cTnC, which were then chronically paced in culture to partially activate calcineurin-NFAT signaling as previously shown (Makarewich et al., 2012). Feline myocytes were used because of their low net cytosolic Ca^{2+} concentrations that reduces baseline NFAT translocation. Increases in pacing frequency caused a significantly greater translocation of NFATc3-GFP into the nucleus in myocytes expressing I61Q cTnC compared with WT cTnC control infection, suggesting that the Ca^{2+} dysregulation by I61Q cTnC enhances calcineurin activity (Figure 6A). Remarkably, L48Q infection also promoted greater NFATc3-GFP translocation in this assay (data not shown, see discussion). With respect to the growth response *in vivo*, I61Q TG mice lacking the catalytic subunit of calcineurin Aβ (*Ppp3cb*$^{-/-}$) were examined for altered cardiac hypertrophy and remodeling. Here, a reduction of calcineurin activity in I61Q TG mice failed to improve systolic function (Figure 6B) or alter LV chamber dilation or septal thickness (Figure 6C–D). However, cardiac mass was reduced to near normal levels suggesting that calcineurin functions as a generalized growth signal in DCM, but does not affect the geometric remodeling of that growth (Figure 6E).

Previous studies identified a role for extracellular signal-related kinase1/2 (ERK1/2) in coordinating long versus short axis myocyte growth through the serial (eccentric growth) or parallel (concentric growth) addition of sarcomeres within individual cardiomyocytes (Bueno et al., 2000; Kehat et al., 2011). To determine if ERK1/2 signaling participates in coordinating the type of geometric growth associated with the I61Q mutation in the heart, isolated adult rat cardiac myocytes were adenovirally transduced with WT or I61Q cTnC and subjected to 48 hours of chronic pacing (2 Hz). Pacing of WT cTnC myocytes caused ERK1/2 to translocate to the nucleus, which was inhibited in the presence of I61Q cTnC mutant (Figure 6F & G). Notably, the retention of ERK1/2 in the cytosol corresponded to a significant increase in I61Q myocyte length while cTnC control infected myocytes remained unchanged (Figure 6H). These results suggest that the I61Q-dependent loss of diastolic tension impairs ERK1/2 signaling and initiates a default pathway for myocyte lengthening hypertrophy (see discussion).

To examine the role of ERK1/2 signaling in the whole heart, TG mice expressing activated MEK1, which directly mediates ERK1/2 activation, were crossed into the I61Q TG background. Surprisingly, MEK1 expression rescued fractional shortening in I61Q mice resulting in hyperdynamic systolic function similar to mice expressing the MEK1 TG alone (Figure 6I). I61Q-MEK1 double TG mice still have ~45% replacement of native cTnC with I61Q cTnC (data not shown), although they now have normal LV chamber dimensions and increased septal and LV wall thicknesses, compared to I61Q TG mice (Figure 6J–L). Importantly, increased ERK1/2 signaling did not change the increase in absolute cardiac mass associated with the I61Q mutation, suggesting that ERK1/2 only directs the type of cardiac geometric growth, not magnitude (Figure 6M).

Developing a Predictive Index of Cardiac Remodeling

Four independent and non-integrated parameters were modeled, such as myocyte shortening, 90% relaxation time, Ca^{2+} transient amplitude, and 90% Ca^{2+} decay time, to potentially predict changes in ventricular mass or chamber size as experimentally measured throughout

this manuscript (Figure S4A–L). However, linear regression analysis of these 4 kinetic- and amplitude-based parameters were unsuccessful in predicting ventricular mass (HW/BW), although mechanical relaxation and Ca^{2+} decay kinetics significantly predicted septal and posterior wall thickness, while mechanical relaxation predicted diastolic dimension (Figure S4E, S4F & S4L).

To generate a more penetrant predictive index, we first normalized the mean twitch (or shortening) and Ca^{2+} transients to WT values, and then calculated an integral value for each, which is the total area under the curve of tension or Ca^{2+}, as a function of time (see methods). This analysis demonstrated that the integrated tension curve predicted all of the remodeling parameters examined here including ventricular mass (Figure S5A–C), which we were unable to predict from non-integrated kinetic or magnitude parameters (Figure S4). By contrast, the integrated Ca^{2+} area was not predictive of any growth parameters used in this analysis suggesting that the myocytes primarily respond to the duration and magnitude of mechanical tension in their growth decisions (Figure S5D–F). This linear regression analysis was further refined by testing the computer-simulated contractions for the I61Q-*Atp2a2*$^{+/-}$ and L48Q-*Atp2a2*$^{+/-}$ crosses, and indeed integrated tension but not Ca^{2+} predicted the changes in ventricular chamber dimension, wall thickness, and cardiac mass observed in these mice (Figure S5A–F).

To simplify the relationships discussed above we assembled the information from these linear regressions into a tension-index that predicts not only the type of cardiac remodeling but also its magnitude. For this refined index, the average integrated tension for the WT/non-diseased condition was valued at 0 equating to no hypertrophic growth. To place genetically manipulated mice on the index, the mean WT/non-diseased force areas were subtracted from their integrated tension values as illustrated with I61Q versus WT in Figure 7A. With this refined index, dilated hypertrophy is represented by negative values while positive values represent concentric hypertrophy. For example, the L48Q mutant scored a positive value on the tension-index with thickening hypertrophy that typifies HCM while the I61Q mutant scored a negative value that yields dilated or eccentric heart growth and DCM (Figure 7B). The magnitude of the value beyond 0 then reflects the severity of cardiac remodeling and hypertrophy.

To demonstrate the predictive breadth of this tension (force) integration method we also assessed an an independent mouse model of DCM derived from a truncation mutation in cardiac troponin T (Δ210 TnT) as well as a restrictive cardiomyopathy (RCM) model from a missense mutation in cardiac troponin I (R193H TnI). The integrated-tension was calculated from the force-time curve data published for Δ210 and non-TG myocytes, which produced a negative score similar to the value obtained for I61Q TG mice (Figure 7C). The restrictive cardiomyopathy-linked mutant R193H TnI, which in mice causes high-end diastolic pressure and no changes in ventricular growth, yielded a positive score that was slightly greater than the L48Q cTnC mutant (Figure 7C).

With the advent of iPSC technology, it is possible to generate cardiomyocytes from patient-derived fibroblasts to directly measure myocyte twitch forces. Here contractile force and Ca^{2+} transients were measured from iPSC-derived cardiomyocytes from 2 HCM and 2 DCM

patients with mutations in the following genes: *MYH7* gene (R663H, HCM) (Lan et al., 2013), *MYBPC3* (R943ter, HCM), *TNNT2* (R173W,DCM) (Sun et al., 2012) and *PLN* (R9C, DCM). Figure S6A–B shows the mean twitch (stress) and Ca^{2+} transients measured across iPSC-derived cardiomyocytes from the genotyped cardiomyopathic and non-diseased patients. The integrated-tension index accurately predicted the known clinical phenotype for each of the patients when normalized to healthy iPSCs-derived cardiomyocytes (Figure 7C). We also examined the predictive ability of the Ca^{2+} integral to align with HCM or DCM phenotypes, and again observed that Ca^{2+} handling alterations failed to correlate with either clinical diagnosis (Figure S6C & S6D).

DISCUSSION

Here we engineered a refined predictive index of cardiac remodeling due to mutations in sarcomeric genes that underlie familial HCM and DCM, in part by collecting experiment data with cTnC variants that shift its Ca^{2+} binding properties and associated myofilament tension dynamics on either side of normal. While *TNNC1* human mutations are rare in humans, they have been attributed to causing HCM or DCM (Kalyva et al., 2014). We also used mutant cTnCs because they represent the proximal Ca^{2+} binding element of the sarcomere, hence allowing for a more direct modulation of the Ca^{2+}-tension relationship without potential confounding effects. The L48Q and I61Q variants used here have been rigorously quantified for their effects on tension and Ca^{2+} handling dynamics (Kreutziger et al., 2011; Parvatiyar et al., 2010; Tikunova and Davis, 2004; Wang et al., 2012; Feest et al., 2014).

Perturbations in the tension dynamic on either side of 0 equally initiated calcineurin-dependent increases in cardiac mass (Figure 7B). Indeed, stimulation-frequency dependent translocation of NFAT to the nucleus was observed with both a gain and loss in myofilament activation. While not tested here, there are several regulators of NFAT translocation and cardiac hypertrophy including glycogen synthase kinase 3β (GSK3β) that may help account for this feature, even in an HCM background (Luckey et al., 2009). Our observations that loss of the *Ppp3cb* gene reduces growth in the I61Q background, but not ventricular remodeling, is consistent with an array of past data in the literature implicating calcineurin-NFAT signaling as a primary determinant of generalized cardiac hypertrophy (Houser and Molkentin, 2008). However, this is not to contend that calcineurin pharmacologic inhibitors, such as cyclosporine A, should be considered as a therapeutic option, as this drug worsened the pathology of R403Q mutant mice (Fatkin et al., 2000).

MEK1-ERK1/2 signaling appears to be responsible for the directionality of cardiac growth by mediating the addition of sarcomeres in parallel to “thicken” cardiomyocytes, while inhibition of MEK-ERK1/2 signaling results in a default program of myocyte elongation due to addition of sarcomeres in series (Kehat et al., 2011). Our model predicts that ERK1/2 signaling is activated in HCM models that have a positive tension integral value, yet inhibited for negative values, such as observed in DCM (Figure 7B). Experimentally, there was minimal nuclear translocation of ERK1/2 in I61Q myocytes, which correlated to *in vivo* dilated growth through myocyte elongation (Figure 6F–H). This effect of I61Q was completely reversed by MEK1 overexpression, which now showed only concentric

remodeling and myocyte thickening, similar to MEK1 alone (Figure 6J–M). Our previous work showed that loss of ERK1/2 from the heart resulted in a program of extreme cardiac dilation due to addition of sarcomeres in series in individual myocytes and their elongation, further indicating that ERK1/2 can be primary signaling determinants underlying the type of cardiac growth that occurs to a given stressed stated (Kehat and Molkentin, 2010; Kehat et al., 2011).

Because L48Q myocytes failed to hypertrophy, we substituted a more potent mutant in the cTnI encoding gene that causes myocyte thickening that arises from increased diastolic tension and pressures in mice (Davis et al., 2007, 2008). Adenoviral transduction-mediated expression of R193H cTnI caused a significant translocation of ERK1/2 to the nucleus in adult rat myocytes (Figure S7A and S7B). This ERK1/2 translocation profile with R193H expression corresponded to reduced myocyte length and increased width at baseline and after chronic pacing (Figure S7C). Co-transduction of R193H cTnI and a dominant negative MEK1 (DnMEK1) encoding adenovirus blocked ERK1/2 translocation and reduced the concentric phenotype observed in R193H myocytes (Figure S7B and S7C). In Figure 7C the tension integral was calculated for this mutant using previously published data (Davis et al., 2007; Davis et al., 2012) and it has a positive remodeling score, indicative of predisposing to HCM. Interestingly the reported patient genotyped with R193H TnI started with a clinical diagnosis of restrictive cardiomyopathy (Mogensen et al., 2003), but later transitioned to HCM, which would have been the initial prediction by our integrated-tension index.

Experimentally correcting for compensation mediated by β-adrenergic drive by chronically administering β-blockers to L48Q mice caused their hearts to concentrically remodel for the first time (Figure 2L & 2N & Figure S2B–D). The net tension integral calculated for L48Q with β-blocker therapy is much higher than either the L48Q or R193H mutations on the thickening hypertrophy spectrum shown in the chart in Figure 7C, suggesting that β-blocker therapy in the mouse causes disease likely due to the very short diastolic window in this species. Use of ivabradine as an independent pharmacologic approach, which similarly slows the contractile cycle producing more net time under tension in the mouse, also produced the same effect as β-blockers in unmasking the concentric hypertrophic potential of the L48Q mutation. Interestingly, apart from possibly reducing arrhythmia-related sudden death in humans with HCM, β-blockers appear to have no protective effect in abating cardiac remodeling and hypertrophy associated with this disease (Hamada et al., 2014; Ostman-Smith, 2010; Spoladore et al., 2012; Tardiff et al., 2015).

Engineering the integrated tension-index not only provided a predictive model of cardiac growth in both mouse and human systems, it has also informed our understanding of pathologic growth in familial cardiomyopathic disease as a mechanically-sensed parameter. This is especially true when considering that the integrated Ca^{2+} transient or any singular Ca^{2+} parameter poorly predicted heart remodeling in the experimental models with direct modulations of contractile Ca^{2+} cycling through the loss of SERCA2 or phospholamban. Moreover, the patient iPSC cardiac myocytes with the R9C PLN mutation also had a Ca^{2+} transient similar to those produced in myocytes derived from healthy iPSCs. The tension based model is also consistent with the observation that non-Ca^{2+} sensitizing mutations in sarcomeric proteins such as titin, co-segregate with cardiomyopathy but only alter tension

(Hinson et al., 2015; LeWinter and Granzier, 2013). Thus we envision that the basic integrated-tension index described here could be used to inform pharmacologic treatment paradigms to achieve the best therapeutic outcome in HCM and DCM patients.

EXPERIMENTAL METHODS

An expanded version of the materials and methods appears in the supplementary data section that accompanies this manuscript.

Computational Simulations of Myocyte Tension and Ca^{2+} Cycling

The computational simulations employed here were performed in the visual basic software environment and constructed by adapting previously reported parameters (Negroni and Lascano, 2008) to our mouse myocyte experimental data in which unloaded and fixed length myocyte twitch tension and the related Ca^{2+} transient are simulated. This model was constructed using Huxley's original contraction model (Huxley, 1957) and incorporating the 3-states of troponin-tropomyosin inhibition of crossbridge cycling.

Predictive Algorithm for Cardiac Growth

To account for methodological differences in measuring twitch shortening or tension and Ca^{2+} cycling, each transient's baseline is set to zero and normalized to the WT or non-diseased condition. The area under the curve is calculated for the mean twitch force per condition.

Linear Regression Analysis of the Integrated-Tension Index

Four non-integrated parameters measured in isolated myocyte contractile assays (mean shortening, 90% relaxation time, Ca^{2+} transient amplitude, and 90% Ca^{2+} decay time) and 2 integrated parameters, which include the areas under the mean twitch (shortening or tension) and Ca^{2+} transient were individually regressed against the following cardiac growth parameters: cardiac mass (HW/BW), ventricular chamber dimension, and wall thickness. The Pearson correlation coefficient (r) and R^2 values were calculated and statistically analyzed by Prism software using a two-tailed test, α=0.05, and n=22.

Mouse Echocardiography and Invasive Hemodynamics

Mice were anesthetized and echocardiography measurements made at the ages described. M-Mode measurements were used to assess fractional shortening, chamber dimensions and wall thickness during systole and diastole. In vivo hemodynamics were measured in anesthetized and ventilated mice using a pressure-volume catheter (1.2F, Transonic System Inc) inserted into the left ventricle through the carotid artery. All experimentation on mice was approved by the Institutional Animal Care and Use Committee of Cincinnati Children's Hospital Medical Center.

Statistics

Unpaired t-tests were used to determine statistical significance in experiments with 2 groups, and a 1-way analysis of variance (ANOVA) was used to determine statistical significance for

multivariate experiments. Pairwise comparisons were made using Newman-Keuls tests (Prism software). All graphed data are represented as mean +/− SEM.

Supplementary Material

Refer to Web version on PubMed Central for supplementary material.

Acknowledgments

This work was supported by grants from the National Institutes of Health (J.D.M., M.R., S.R.H., C.E.S., J.G.S., J.M.M, J.C.W. and J.D, and by the Howard Hughes Medical Institute (to J.D.M. and C.E.S.)

References

Bers DM. Cardiac excitation-contraction coupling. Nature. 2002; 415:198–205. [PubMed: 11805843]

Bueno OF, De Windt LJ, Tymitz KM, Witt SA, Kimball TR, Klevitsky R, Hewett TE, Jones SP, Lefer DJ, Peng CF, et al. The MEK1-ERK1/2 signaling pathway promotes compensated cardiac hypertrophy in transgenic mice. EMBO J. 2000; 19:6341–6350. [PubMed: 11101507]

Davis J, Metzger JM. Combinatorial effects of double cardiomyopathy mutant alleles in rodent myocytes: a predictive cellular model of myofilament dysregulation in disease. PLoS One. 2010; 5:e9140. [PubMed: 20161772]

Davis J, Wen H, Edwards T, Metzger JM. Thin filament disinhibition by restrictive cardiomyopathy mutant R193H troponin I induces Ca2+-independent mechanical tone and acute myocyte remodeling. Circ Res. 2007; 100:1494–1502. [PubMed: 17463320]

Davis J, Wen H, Edwards T, Metzger JM. Allele and species dependent contractile defects by restrictive and hypertrophic cardiomyopathy-linked troponin I mutants. J Mol Cell Cardiol. 2008; 44:891–904. [PubMed: 18423659]

Davis J, Yasuda S, Palpant NJ, Martindale J, Stevenson T, Converso K, Metzger JM. Diastolic dysfunction and thin filament dysregulation resulting from excitation-contraction uncoupling in a mouse model of restrictive cardiomyopathy. J Mol Cell Cardiol. 2012; 53:446–457. [PubMed: 22683325]

Fatkin D, Graham RM. Molecular mechanisms of inherited cardiomyopathies. Physiol Rev. 2002; 82:945–980. [PubMed: 12270949]

Fatkin D, McConnell BK, Mudd JO, Semsarian C, Moskowitz IG, Schoen FJ, Giewat M, Seidman CE, Seidman JG. An abnormal Ca(2+) response in mutant sarcomere protein-mediated familial hypertrophic cardiomyopathy. J Clin Invest. 2000; 106:1351–1359. [PubMed: 11104788]

Feest ER, Steven Korte F, Tu AY, Dai J, Razumova MV, Murry CE, Regnier M. Thin filament incorporation of an engineered cardiac troponin C variant (L48Q) enhances contractility in intact cardiomyocytes from healthy and infarcted hearts. J Mol Cell Cardiol. 2014; 72:219–227. [PubMed: 24690333]

Geisterfer-Lowrance AA, Christe M, Conner DA, Ingwall JS, Schoen FJ, Seidman CE, Seidman JG. A mouse model of familial hypertrophic cardiomyopathy. Science. 1996; 272:731–734. [PubMed: 8614836]

Gordon AM, Homsher E, Regnier M. Regulation of contraction in striated muscle. Physiol Rev. 2000; 80:853–924. [PubMed: 10747208]

Hamada M, Ikeda S, Shigematsu Y. Advances in medical treatment of hypertrophic cardiomyopathy. J Cardiol. 2014; 64:1–10. [PubMed: 24735741]

Hinson JT, Chopra A, Nafissi N, Polacheck WJ, Benson CC, Swist S, Gorham J, Yang L, Schafer S, Sheng CC, et al. HEART DISEASE. Titin mutations in iPS cells define sarcomere insufficiency as a cause of dilated cardiomyopathy. Science. 2015; 349:982–986. [PubMed: 26315439]

Houser SR, Molkentin JD. Does contractile Ca2+ control calcineurin-NFAT signaling and pathological hypertrophy in cardiac myocytes? Sci Signal. 2008; 1:pe31. [PubMed: 18577756]

Huxley AF. Muscle structure and theories of contraction. Prog Biophys Biophys Chem. 1957; 7:255–318. [PubMed: 13485191]

Kalyva A, Parthenakis FI, Marketou ME, Kontaraki JE, Vardas PE. Biochemical characterisation of Troponin C mutations causing hypertrophic and dilated cardiomyopathies. J Muscle Res Cell Motil. 2014; 35:161–178. [PubMed: 24744096]

Kehat I, Davis J, Tiburcy M, Accornero F, Saba-El-Leil MK, Maillet M, York AJ, Lorenz JN, Zimmermann WH, Meloche S, et al. Extracellular signal-regulated kinases 1 and 2 regulate the balance between eccentric and concentric cardiac growth. Circ Res. 2011; 108:176–183. [PubMed: 21127295]

Kehat I, Molkentin JD. Molecular pathways underlying cardiac remodeling during pathophysiological stimulation. Circulation. 2010; 122:2727–2735. [PubMed: 21173361]

Kreutziger KL, Piroddi N, McMichael JT, Tesi C, Poggesi C, Regnier M. Calcium binding kinetics of troponin C strongly modulate cooperative activation and tension kinetics in cardiac muscle. J Mol Cell Cardiol. 2011; 50:165–174. [PubMed: 21035455]

Lan F, Lee AS, Liang P, Sanchez-Freire V, Nguyen PK, Wang L, Han L, Yen M, Wang Y, Sun N, et al. Abnormal calcium handling properties underlie familial hypertrophic cardiomyopathy pathology in patient-specific induced pluripotent stem cells. Cell Stem Cell. 2013; 12:101–113. [PubMed: 23290139]

LeWinter MM, Granzier HL. Titin is a major human disease gene. Circulation. 2013; 127:938–944. [PubMed: 23439446]

Luckey SW, Walker LA, Smyth T, Mansoori J, Messmer-Kratzsch A, Rosenzweig A, Olson EN, Leinwand LA. The role of Akt/GSK-3beta signaling in familial hypertrophic cardiomyopathy. J Mol Cell Cardiol. 2009; 46:739–747. [PubMed: 19233194]

Makarewich CA, Correll RN, Gao H, Zhang H, Yang B, Berretta RM, Rizzo V, Molkentin JD, Houser SR. A caveolae-targeted L-type Ca(2)+ channel antagonist inhibits hypertrophic signaling without reducing cardiac contractility. Circ Res. 2012; 110:669–674. [PubMed: 22302787]

McNally EM, Golbus JR, Puckelwartz MJ. Genetic mutations and mechanisms in dilated cardiomyopathy. J Clin Invest. 2013; 123:19–26. [PubMed: 23281406]

Metzger JM, Westfall MV. Covalent and noncovalent modification of thin filament action: the essential role of troponin in cardiac muscle regulation. Circ Res. 2004; 94:146–158. [PubMed: 14764650]

Michele DE, Gomez CA, Hong KE, Westfall MV, Metzger JM. Cardiac dysfunction in hypertrophic cardiomyopathy mutant tropomyosin mice is transgene-dependent, hypertrophy-independent, and improved by beta-blockade. Circ Res. 2002; 91:255–262. [PubMed: 12169652]

Mogensen J, Kubo T, Duque M, Uribe W, Shaw A, Murphy R, Gimeno JR, Elliott P, McKenna WJ. Idiopathic restrictive cardiomyopathy is part of the clinical expression of cardiac troponin I mutations. J Clin Invest. 2003; 111:209–216. [PubMed: 12531876]

Negroni JA, Lascano EC. Simulation of steady state and transient cardiac muscle response experiments with a Huxley-based contraction model. J Mol Cell Cardiol. 2008; 45:300–312. [PubMed: 18550079]

Ostman-Smith I. Hypertrophic cardiomyopathy in childhood and adolescence - strategies to prevent sudden death. Fundam Clin Pharmacol. 2010; 24:637–652. [PubMed: 20727015]

Parvatiyar MS, Pinto JR, Liang J, Potter JD. Predicting cardiomyopathic phenotypes by altering Ca2+ affinity of cardiac troponin C. J Biol Chem. 2010; 285:27785–27797. [PubMed: 20566645]

Shettigar V, Zhang B, Little SC, Salhi HE, Hansen BJ, Li N, Zhang J, Roof SR, Ho HT, Brunello L, et al. Rationally engineered Troponin C modulates in vivo cardiac function and performance in health and disease. Nat Commun. 2016; 7:10794. [PubMed: 26908229]

Spoladore R, Maron MS, D'Amato R, Camici PG, Olivotto I. Pharmacological treatment options for hypertrophic cardiomyopathy: high time for evidence. Eur Heart J. 2012; 33:1724–1733. [PubMed: 22719025]

Sun N, Yazawa M, Liu J, Han L, Sanchez-Freire V, Abilez OJ, Navarrete EG, Hu S, Wang L, Lee A, et al. Patient-specific induced pluripotent stem cells as a model for familial dilated cardiomyopathy. Sci Transl Med. 2012; 4:130ra147.

Tardiff JC, Carrier L, Bers DM, Poggesi C, Ferrantini C, Coppini R, Maier LS, Ashrafian H, Huke S, van der Velden J. Targets for therapy in sarcomeric cardiomyopathies. Cardiovasc Res. 2015; 105:457–470. [PubMed: 25634554]

Tikunova SB, Davis JP. Designing calcium-sensitizing mutations in the regulatory domain of cardiac troponin C. J Biol Chem. 2004; 279:35341–35352. [PubMed: 15205455]

Wang D, Robertson IM, Li MX, McCully ME, Crane ML, Luo Z, Tu AY, Daggett V, Sykes BD, Regnier M. Structural and functional consequences of the cardiac troponin C I61Q Ca(2+)-sensitizing mutation. Biochemistry. 2012; 51:4473–3387. [PubMed: 22591429]

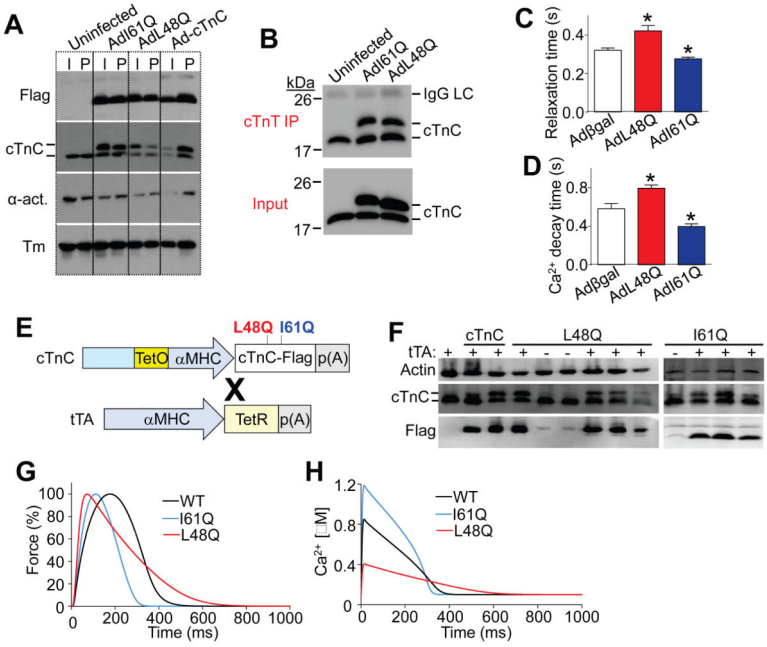

Figure 1. Ca^{2+} Binding Properties of cTnC Variants Alter Myocyte Tension and Ca^{2+} Dynamics

(A) Western blot analysis against Flag, cTnC, α-actinin (α-act.) and tropomyosin (Tm) in protein lysates from adenovirally transduced adult rat cardiac myocytes 3 days after gene transfer. Tm and α-act were loading controls. The cTnC antibody shows the slower migrating Flag epitope-tagged cTnC constructs that were overexpressed and endogenous cTnC. Samples were processed from intact (I) and permeabilized (P) myocytes to show sarcomeric incorporation.

(B) Cardiac TnC western blot after co-immunoprecipitation (IP) with anti-cTnT from adult rat cardiac myocytes that were untreated or adenovirally transduced with L48Q cTnC-Flag (AdL48Q) or I61Q cTnC-Flag (AdI61Q) as a further control for the data shown in panel A. Abbreviation; IgG LC, Mouse IgG light chain.

(C) Graph showing 75% mechanical relaxation time in paced isolated adult rat cardiac myocytes adenovirally transduced with βgal, L48Q cTnC, and I61Q cTnC. Error bars represent the mean+SEM, n=40 myocytes distributed across 3 preparations, *P<0.05 vs βgal adenoviral infection

(D) Graph showing 75% Ca^{2+} transient decay time in paced isolated adult rat cardiac myocytes adenovirally transduced with βgal, L48Q cTnC, and I61Q cTnC. Error bars represent the mean+SEM, n=40 myocytes distributed across 3 preparations, *P<0.05 vs βgal adenoviral infection

(E) A schematic depicting the bi-transgenic (TG) system used for cardiac-specific expression of WT, L48Q, or I61Q cTnC with a carboxy-terminal Flag epitope directed by the αMHC-promoter. Abbreviations; tTA, tetracycline transactivator construct; TetR, tetracycline repressor protein; p(A), polyadenylation signal; TetO, Tetracycline operator sequence.

(F) Western blots with an anti-cTnC and anti-Flag antibody demonstrating the relative expression of epitope-tagged WT, L48Q, and I61Q cTnC versus faster migrating

endogenous cTnC in the presence or absence of the tTA transgene. Actin was a loading control.

(G) Computationally derived Ca^{2+}-activated unloaded twitch force over time of a single contraction in simulated myocytes expressing WT (black), L48Q (red), and I61Q (blue) cTnC.

(H) Computationally derived Ca^{2+} transients over time of a single contraction in simulated myocytes expressing WT (black), L48Q (red), and I61Q (blue) cTnC.

Also see Figure S1.

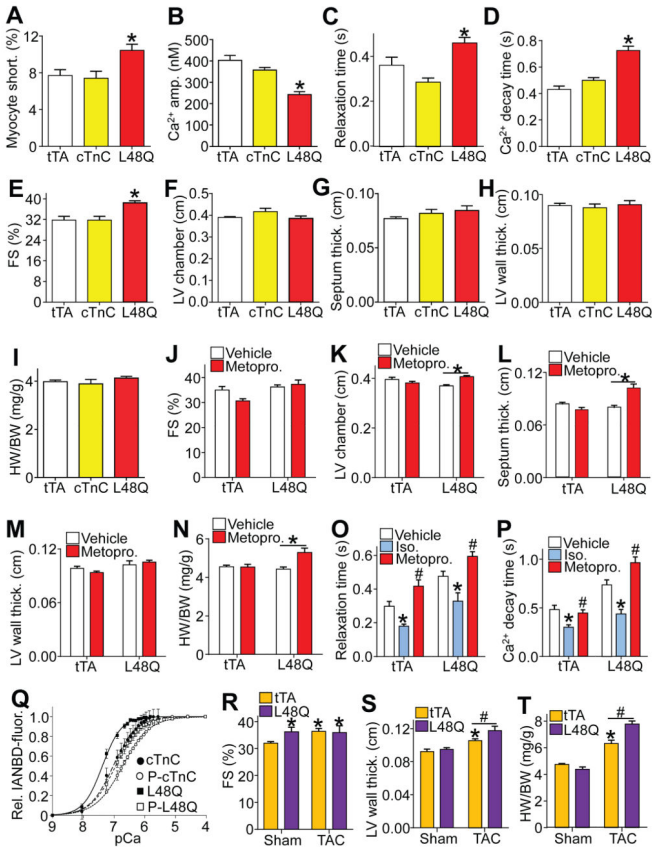

Figure 2. Increased Ca^{2+} Binding and Prolonged Tension by L48Q cTnC Causes Concentric Hypertrophy

(A–D) Average percent shortening, (B) Ca^{2+} transient amplitude, (C) 75% myocyte relaxation time, and (D) 75% Ca^{2+} transient decay time measured in myocytes isolated from TG tTA only controls or WT cTnC and L48Q cTnC hearts. Error bars represent the mean +SEM, n>43 myocytes distributed across 3–5 preparations per experimental group, *P<0.05 vs tTA, WT cTnC.

(E–H) Average myocardial fractional shortening (FS), (F) left ventricular (LV) diastolic chamber dimension, (G) septal wall thickness, and (H) posterior LV wall thickness measured by M-mode echocardiography in 3 month-old tTA, WT cTnC, and L48Q cTnC TG mice. Error bars represent the mean+SEM, n=8–10 mice per group, *P<0.05 vs tTA, WT cTnC.

(I) Average heart-weight normalized to body-weight (HW/BW) in the indicated groups of mice. Error bars represent the mean+SEM, n=8–10 mice per group.

(J–M) Average myocardial FS, (K) LV diastolic chamber dimension, (L) septal wall thickness, and (M) LV posterior wall thickness measured by M-mode echocardiography with vehicle or chronic β-blocker (metopro.) delivery in tTA and L48Q cTnC TG mice. Error bars represent the mean+SEM, n=7–8 mice per group, *P<0.05 vs L48Q+vehicle.

(N) Average HW/BW for the indicated groups of mice treated with vehicle or metoprolol. Error bars represent the mean+SEM, n=7–8 mice per group, *P<0.05 vs L48Q+vehicle.

(O,P) Average 75% myocyte relaxation time, and (P) 75% Ca^{2+} transient decay time in myocytes isolated from tTA and L48Q cTnC TG hearts acutely perfused with vehicle,

isoproterenol (Iso.), or metoprolol (metopro.). Error bars represent the mean+SEM, n=25 myocytes across 3 preparations. *P<0.05 isoproterenol effect, #P<0.05 metoprolol effect.
(Q) Effects of L48Q mutation on Ca^{2+} binding by cTnC alone or complexed with phosphorylated cTnI. Changes in the fluorescence intensities of the environmentally sensitive probe IANBD labeled $cTnC^{C35S}$ measured in response to increasing Ca^{2+} concentrations. The error bars represent the SEM, n=3.
(R–T) The effect of transverse aortic constriction (TAC) or a sham procedure on myocardial FS, (S) posterior wall thickness, and (T) HW/BW in tTA or L48Q TG mice. Bars represent the mean+SEM, n=5–8 mice per group, *P<0.05 vs tTA-Sham; #P<0.05 vs tTA TAC.
Also see Figure S2.

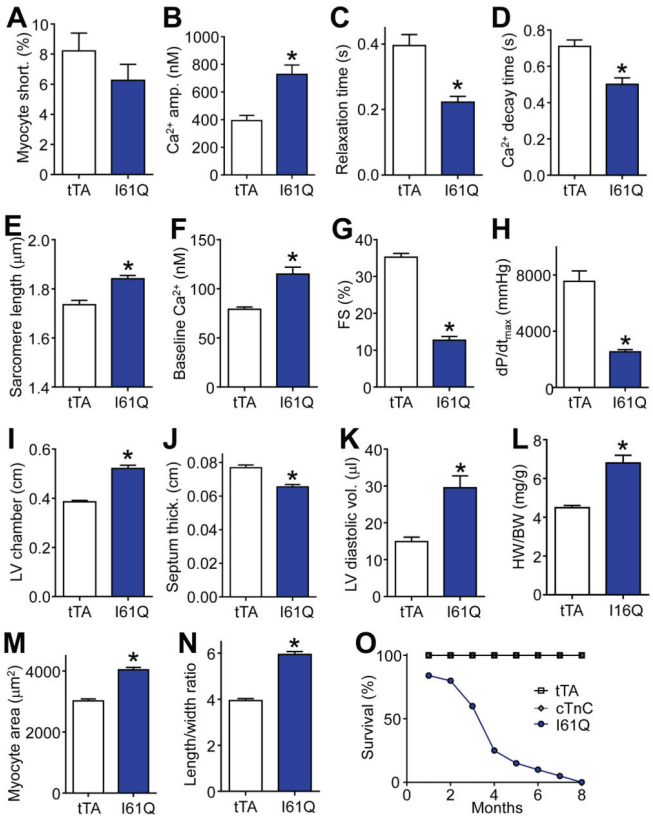

Figure 3. Reduced Ca^{2+} Binding and Tension by I61Q cTnC Causes Eccentric Hypertrophy

(A–F) Average percent shortening, (B) Ca^{2+} transient amplitude, (C) 75% myocyte relaxation time, (D) 75% Ca^{2+} transient decay time, (E) diastolic sarcomere length, and (F) diastolic Ca^{2+} measured in myocytes isolated from tTA or I61Q cTnC TG hearts. Error bars represent the mean+SEM, n>40 myocytes distributed across 3 preparations per group, *P<0.05 vs tTA.

(G) Average myocardial FS measured by M-mode echocardiography in tTA and I61Q cTnC TG mice at 3 months of age. Error bars represent the mean+SEM, n=8 mice per group, *P<0.05 vs tTA.

(H) Average systolic pressure derivatives over time to assess cardiac contractility as measured by pressure-volume catheterization in the indicated groups of mice. Error bars represent the mean+SEM, n=5 mice per group, *P<0.05 vs tTA.

(I,J) Left ventricular (LV) diastolic chamber dimension and (J) septal wall thickness measured by M-mode echocardiography in tTA and I61Q cTnC TG mice at 3 months of age. Error bars represent the mean+SEM, n=8 mice per group, *P<0.05 vs tTA.

(K) Average LV end diastolic volumes measured by pressure-volume catheterization in the indicated groups of mice. Error bars represent the mean+SEM, n=5 mice per group, *P<0.05 vs tTA.

(L) Average HW/BW in the indicated groups of mice at 3 months of age. Error bars represent the mean+SEM, n=8 mice per group, *P<0.05 vs tTA.

(M,N) Average area and (N) length/width ratios measured in myocytes isolated from tTA and I61Q TG hearts at 3 months of age. Error bars represent the mean+SEM, n=165 myocytes per group, *P<0.05 vs tTA.
(O) Survival curves for tTA, WT cTnC, and I61Q cTnC TG mice. n=12 per group.

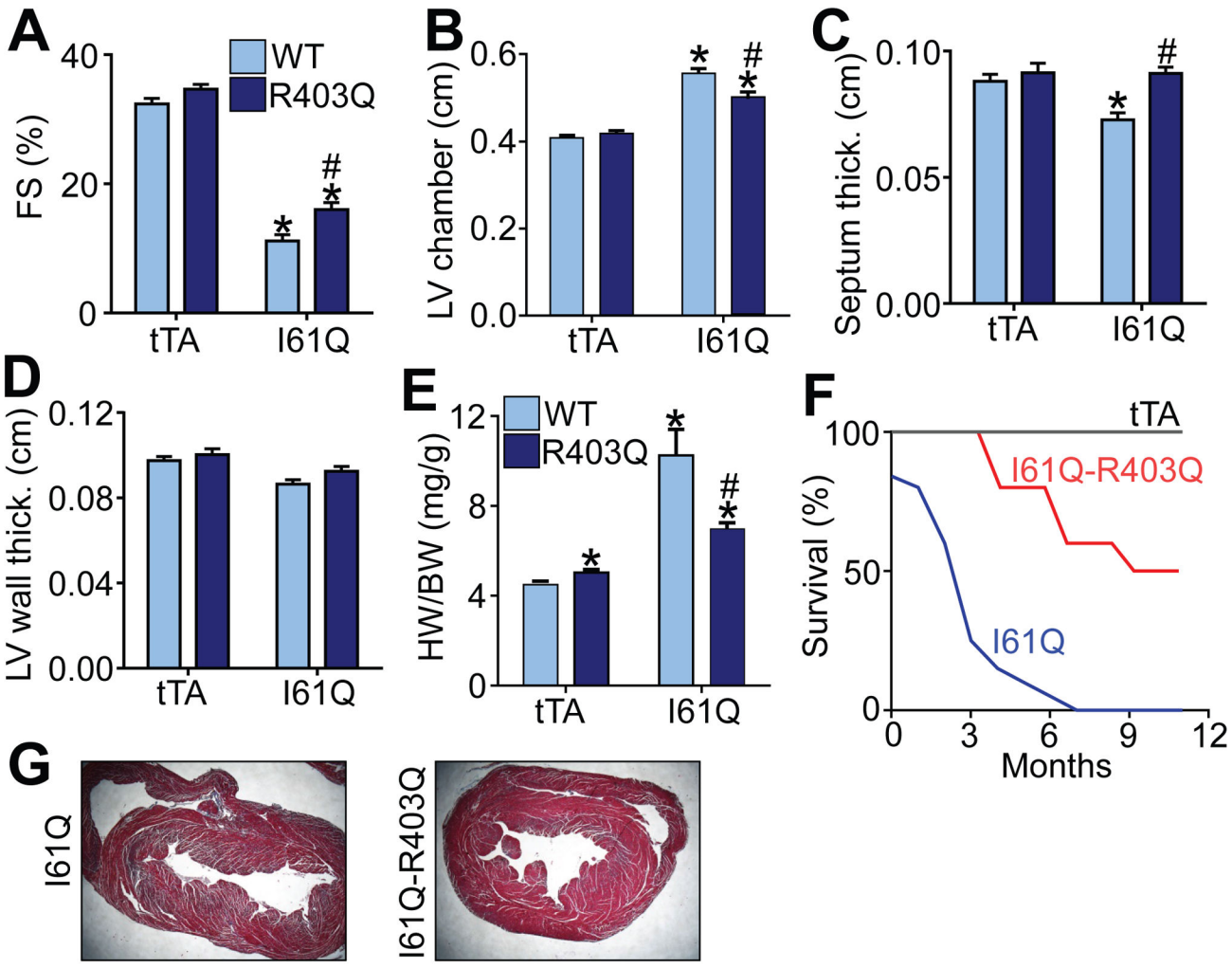

Figure 4. Increased Crossbridge Binding in *Myh6* R403Q Mice Corrects I61Q cTnC-Dependent Eccentric Hypertrophy

(A–D) Average myocardial FS, (B) LV diastolic chamber dimension, (C) septal and (D) LV posterior wall thickness measured by M-mode echocardiography in tTA and I61Q TG mice, some of which were heterozygous for R403Q mutant *Myh6* allele, at 4 months of age. Error bars represent the mean+SEM, n=6–8 mice per group, *P<0.05 vs tTA+WT, #P<0.05 vs. I61Q WT.

(E) Average HW/BW in the indicated mice at 4 months of age. Error bars represent the mean+SEM, n=6–8 mice per group, *P<0.05 vs tTA+WT, #P<0.05 vs. I61Q WT.

(F) Survival curves for tTA, WT cTnC, and I61Q cTnC TG mice with or without the heterozygous R403Q mutation in *Myh6*. n=8 per group.

(G) Representative Masson's Trichrome-stained images of transverse histological sections of hearts from I61Q and I61Q+R403Q$^{+/-}$ mice at 4 months of age. Magnification is 20X.

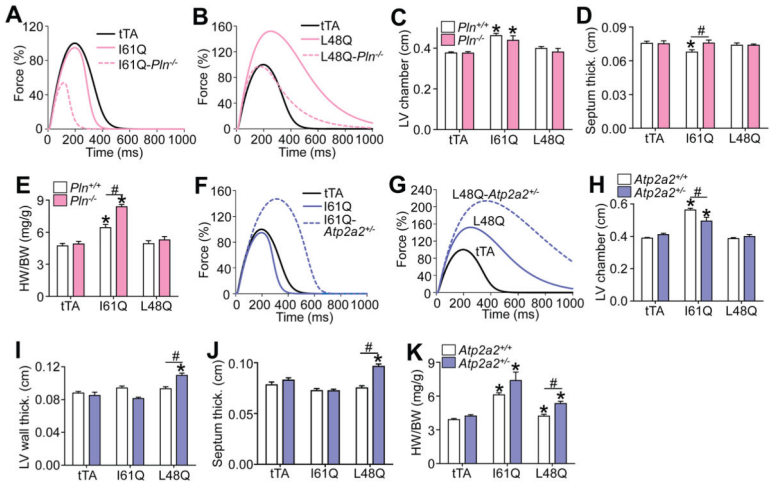

Figure 5. Controlled Alterations in Ca^{2+} Cycling in I61Q and L48Q Mice

(A) Computationally simulated unloaded twitch force in cardiomyocytes expressing either tTA (WT condition), I61Q cTnC, or I61Q cTnC with increased cytosolic Ca^{2+} clearance mediated by loss of phospholamban (I61Q-$Pln^{-/-}$).

(B) Computationally simulated unloaded twitch force in cardiomyocytes expressing either tTA (WT condition), L48Q cTnC, or L48Q cTnC with increased cytosolic Ca^{2+} clearance mediated by loss of phospholamban (L48Q-$Pln^{-/-}$).

(C,D) LV diastolic chamber dimension and (D) septal wall thickness measured by M-mode echocardiography in tTA, I61Q, and L48Q TG mice with or without *Pln* deletion. Error bars represent the mean+SEM, n=6–8 mice per group, *P<0.05 vs tTA+$Pln^{+/+}$, #P<0.05 for 2 conditions shown

(E) Average HW/BW of the depicted groups. Error bars represent the mean+SEM, n=6–8 mice per group, *P<0.05 vs tTA+$Pln^{+/+}$, #P<0.05 for 2 conditions shown.

(F) Computationally simulated unloaded twitch force in cardiomyocytes expressing either tTA (WT condition), I61Q cTnC, or I61Q cTnC with decreased cytosolic Ca^{2+} clearance due to the loss of 1 allele of the gene encoding SERCA2a (I61Q-$Atp2a2^{+/-}$).

(G) Computationally simulated unloaded twitch force in cardiomyocytes expressing either tTA (WT condition), L48Q cTnC, or L48Q cTnC with decreased cytosolic Ca^{2+} clearance due to the loss of 1 allele of the gene encoding SERCA2a (L48Q- $Atp2a2^{+/-}$).

(H–J) LV diastolic chamber dimension, (I) LV wall thickness, and (J) septal thickness measured by M-Mode echocardiography in tTA, I61Q, and L48Q TG mice replete with SERCA2a ($Atp2a2^{+/+}$) or lacking 1 allele of SERCA2a ($Atp2a2^{+/-}$). Error bars represent the mean+SEM, n=6–8 mice per group, *P<0.05 vs tTA+$Atp2a2^{+/+}$, #P<0.05 the 2 conditions shown

(K) Average HW/BW of the depicted groups. Error bars represent the mean+SEM, n=6–8 mice per group, *P<0.05 vs tTA+$Atp2a2^{+/+}$, #P<0.05 for the 2 conditions shown

Also see Figure S1 and S3

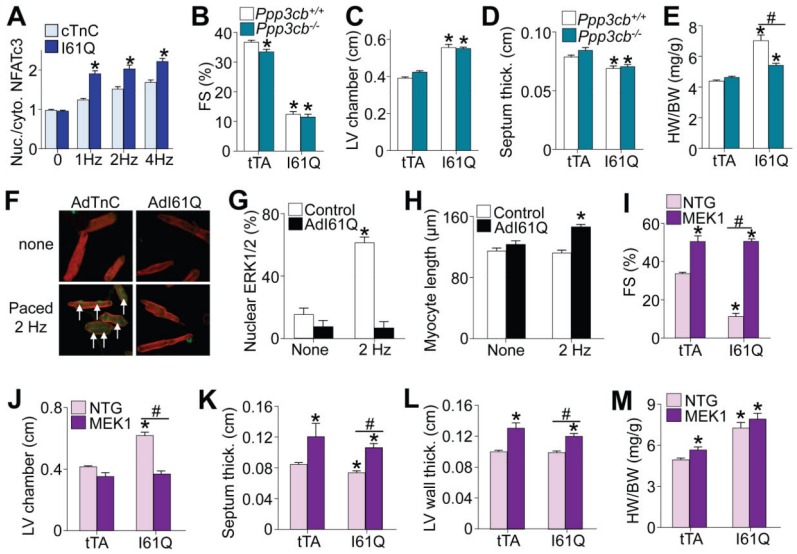

Figure 6. HCM versus DCM Growth Is Regulated by Calcineurin and ERK1/2 Signaling

(A) Ratio of nuclear to cytosolic NFATc3-GFP measured at baseline (0 Hz) and after pacing at the depicted frequencies in isolated feline adult cardiomyocytes adenovirally transduced with WT cTnC or I61Q cTnC. Bars represent the mean+SEM, n=25–59 myocytes per group, *P<0.05 vs WT cTnC.

(B–D) Average FS, (C) LV diastolic chamber dimension, and (D) septal wall thickness measured by M-mode echocardiography in 3 month-old tTA and I61Q cTnC TG mice with (*Ppp3cb*$^{+/+}$) or without calcineurin Aβ (*Ppp3cb*$^{-/-}$). Error bars represent the mean+SEM, n=6–8 mice per group, *P<0.05 vs tTA + *Ppp3cb*$^{+/+}$.

(E) Average HW/BW of the depicted groups at 3 months of age. Error bars represent the mean+SEM, n=6–8 mice per group, *P<0.05 vs tTA + *Ppp3cb*$^{+/+}$, #P<0.05 for the 2 conditions shown.

(F) Representative confocal images of isolated adult rat cardiomyocytes labeled for ERK1/2 (green) and sarcomeric actin (red), which were adenovirally transduced with WT cTnC or I61Q cTnC, with or without 48 hours of pacing. White arrows indicate ERK1/2 translocation into the nucleus after pacing with only WT cTnC. Magnification = 600X.

(G) Quantification of myocytes with nuclear versus cytosolic ERK1/2 from the type of experiment depicted in panel F. Error bars represent the mean+SEM, n=125–135 myocytes per group across 3 preparations, *P<0.05 vs control + no pacing.

(H) Average length of isolated adult rat cardiomyocytes adenovirally transduced with WT cTnC or I61Q cTnC, with or without 48 hours of pacing. Error bars represent the mean +SEM, n=25–35 myocytes per group across 3 preparations, *P<0.05 vs control + no pacing.

(I–L) Average myocardial FS, (J) LV diastolic chamber dimension, (K) septal wall thickness, and (L) LV wall thickness measured by M-mode echocardiography in 3 month-old tTA and I61Q cTnC TG mice with or without a constitutively active MEK1 transgene. Error bars represent the mean+SEM, n=6 mice per group, *P<0.05 vs NTG, #P<0.05 for the 2 conditions shown.

(M) Average HW/BW of the depicted groups. Bars represent the mean+SEM, n=6 mice per group, *P<0.05 vs NTG tTA.

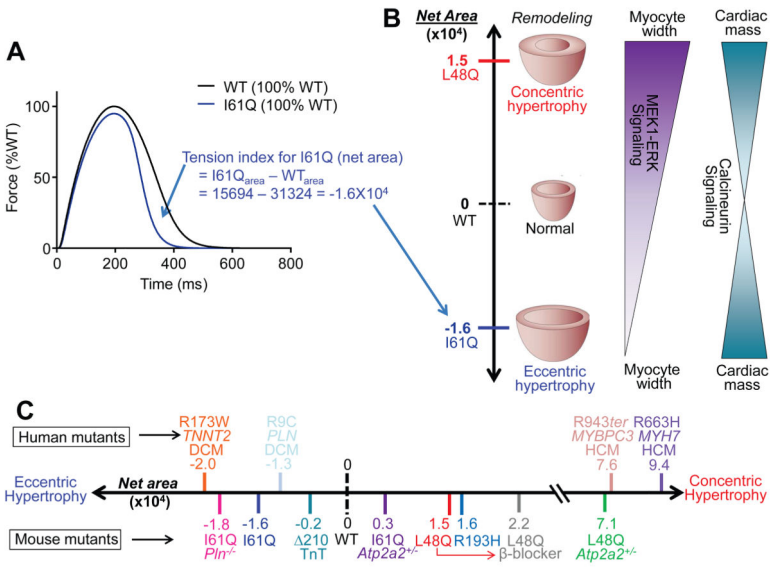

Figure 7. A Predictive Model of Cardiac Growth For Familial Cardiomyopathy-linked Mutations

(A) Mean twitch tensions (shortening) measured in mouse myocytes for I61Q (blue) and WT (black) that were normalized to the WT's mean peak twitch amplitude. Calculation of the tension-index for the I61Q mutant is depicted in blue text in which WT integrated tension (WT_{area}) is subtracted from I61Q integrated tension ($I61Q_{area}$) and the resulting value is the net area placed on the hypertrophic growth continuum depicted in B and C.

(B) Net integrated tension shown in panel A as a line chart with WT being 0, and the I61Q having a negative total value of -1.6×10^4 that predicts dilated heart growth and L48Q being a positive value of $+1.5\times10^4$ predicting thickening hypertrophy. ERK1/2 signaling is reduced by more negative values, which reduces myocyte width but increased with positive values leading to thickening growth. Calcineurin signaling is lowest at 0, yet increased by both positive and negative values.

(C) The same integrated tension as depicted in panel B expanded to include the predicted scores for other sarcomeric mutations in mice (below the line), and from four patients clinically diagnosed with either HCM or DCM (2 each, above the line). The magnitude of the value reflects the degree of disease severity as either concentric hypertrophy (HCM remodeling) or dilated, eccentric (DCM) growth.

Also see Figure S4, S5, S6 and S7